(Figs. 1A and 2). The α4-β6 loop is in close proximity to the COOH-terminus of α5. The contact is stabilized by insertion of Met^{386} into a hydrophobic pocket formed by the NH_2-terminal residues of β5 and β6. Together, the α4-β6 loop and the α5 helix form a plane on the back side of $G_{s\alpha}$ that may interact with receptors (*29–31*). In contrast, the corresponding α5 helix in $G_{i\alpha}$ (as visualized in the structures of the $G_{i\alpha 1}$·GDP·$\beta_1\gamma_2$ and $G_{i\alpha 1}$·GDP·AlF_4^-·RGS4 complexes) is relatively straight and extends away from the central β sheet of the Ras-like domain (Fig. 2). The relative position of the α4-β6 loop of $G_{s\alpha}$ also differs from that of the cognate loop of $G_{i\alpha}$. The divergence of these two structural elements from those of $G_{i\alpha}$ and $G_{t\alpha}$ may therefore contribute to receptor selectivity.

REFERENCES AND NOTES

1. E. J. Neer, *Cell* **80**, 249 (1995).
2. S. R. Sprang, *Annu. Rev. Biochem.* **66**, 639 (1997).
3. R. K. Sunahara, C. W. Dessauer, A. G. Gilman, *Annu. Rev. Pharmacol. Toxicol.* **36**, 461 (1996).
4. D. M. Berman and A. G. Gilman, *J. Biol. Chem.*, in press.
5. J. J. G. Tesmer, R. K. Sunahara, A. G. Gilman, S. R. Sprang, *Science* **278**, 1907 (1997).
6. J. P. Noel, H. E. Hamm, P. B. Sigler, *Nature* **366**, 654 (1993).
7. D. E. Coleman *et al.*, *Science* **265**, 1405 (1994).
8. D. Cassel and Z. Selinger, *Proc. Natl. Acad. Sci. U.S.A.* **74**, 3307 (1977).
9. C. Van Dop, M. Tsubokawa, H. R. Bourne, J. Ramachandran, *J. Biol. Chem.* **259**, 696 (1984).
10. J. Lyons *et al.*, *Science* **249**, 655 (1990).
11. A. M. Spiegel, *Annu. Rev. Physiol.* **58**, 143 (1996).
12. T. Iiri, P. Herzmark, J. M. Nakamoto, C. Van Dop, H. R. Bourne, *Nature* **371**, 164 (1994).
13. Z. Farfel *et al.*, *J. Biol. Chem.* **271**, 19653 (1996).
14. D. R. Benjamin, D. W. Markby, H. R. Bourne, I. D. Kuntz, *J. Mol. Biol.* **254**, 681 (1995).
15. M. A. Wall *et al.*, *Cell* **80**, 1047 (1995).
16. D. G. Lambright *et al.*, *Nature* **379**, 311 (1996).
17. J. J. G. Tesmer, D. M. Berman, A. G. Gilman, S. R. Sprang, *Cell* **89**, 251 (1997).
18. J. Sondek, D. G. Lambright, J. P. Noel, H. E. Hamm, P. B. Sigler, *Nature* **372**, 276 (1994).
19. H. Itoh and A. G. Gilman, *J. Biol. Chem.* **266**, 16226 (1991).
20. C. H. Berlot and H. R. Bourne, *Cell* **68**, 911 (1992).
21. G. Grishina and C. H. Berlot, *J. Biol. Chem.* **272**, 20619 (1997).
22. R. Taussig, W.-J. Tang, J. R. Hepler, A. G. Gilman, *ibid.* **269**, 6093 (1994).
23. T. Iiri, Z. Farfel, H. R. Bourne, *Proc. Natl. Acad. Sci. U.S.A.* **94**, 5656 (1997).
24. C. W. Dessauer, T. T. Scully, A. G. Gilman, *J. Biol. Chem.* **272**, 22272 (1997).
25. A. G. Gilman, *Annu. Rev. Biochem.* **56**, 615 (1987).
26. H. R. Bourne, *Curr. Opin. Struct. Biol.* **9**, 134 (1997).
27. R. Onrust *et al.*, *Science* **275**, 381 (1997).
28. O. Lichtarge, H. R. Bourne, F. E. Cohen, *Proc. Natl. Acad. Sci. U.S.A.* **93**, 7507 (1996).
29. B. R. Conklin and H. R. Bourne, *Cell* **73**, 631 (1993).
30. S. B. Masters *et al.*, *Science* **241**, 448 (1988).
31. M. M. Rasenick, M. Watanabe, M. B. Lazarevic, S. Hatta, H. E. Hamm, *J. Biol. Chem.* **269**, 21519 (1994).
32. E. Lee, M. E. Linder, A. G. Gilman, *Methods Enzymol.* **237**, 146 (1994).
33. Z. Otwinowski, in *Data Collection and Processing*, N. I. L. Sawyer and S. W. Bailey, Eds. (Science and Engineering Council, Daresbury Laboratory, Daresbury, UK, 1993), pp. 56–62.
34. J. Navaza, *Acta Crystallogr.* **A50**, 157 (1994).
35. S. Bailey, *ibid.* **D50**, 760 (1994).
36. T. A. Jones, J.-Y. Zou, S. W. Cowan, *ibid.* **A47**, 110 (1991).
37. A. T. Brünger, A. Krukowski, J. W. Erickson, *ibid.* **A46**, 585 (1990).
38. A. T. Brünger, X-PLOR Version 3.1 (Yale Univ. Press, New Haven, CT, 1992).
39. R. A. Laskowski, M. W. MacArthur, D. S. Moss, J. M. Thornton, *J. Appl. Crystallogr.* **26**, 283 (1993).
40. P. J. Kraulis, *ibid.* **24**, 946 (1991).
41. E. A. Merritt and M. E. P. Murphy, *Acta Crystallogr.* **D50**, 869 (1994).
42. Single-letter abbreviations for the amino acid residues are as follows: A, Ala; C, Cys; D, Asp; E, Glu; F, Phe; G, Gly; H, His; I, Ile; K, Lys; L, Leu; M, Met; N, Asn; P, Pro; Q, Gln; R, Arg; S, Ser; T, Thr; V, Val; W, Trp; and Y, Tyr.
43. A. Nicholls, K. A. Sharp, B. Honig, *Proteins* **11**, 281 (1991).

44. We thank J. Collins for superb technical assistance; C. Kleuss (Frie University, Berlin) for supplying $G_{s\alpha}$-H6 cDNA; B. Posner and D. Coleman for helpful discussion; D. Coleman, T. Harrell, T. Xiao, and the MacCHESS staff for their assistance with data collection at CHESS; and L. Esser for his assistance in preparing figures. R.K.S. was supported by a postdoctoral fellowship from the Medical Research Council of Canada. This work was supported by NIH grant DK46371 and Welch Foundation grant I-1229 to S.R.S. and by NIH grant GM34497, American Cancer Society grant RPG-77-001-21-BE, Welch Foundation grant I-1271, and the Raymond and Ellen Willie Distinguished Chair of Molecular Neuropharmacology to A.G.G. Atomic coordinates have been deposited with the Protein Data Bank (1AZT).

24 October 1997; accepted 14 November 1997

Mediation of Sonic Hedgehog–Induced Expression of COUP-TFII by a Protein Phosphatase

Venkatesh Krishnan, Fred A. Pereira, Yuhong Qiu, Chien-Huan Chen, Philip A. Beachy, Sophia Y. Tsai,* Ming-Jer Tsai*†

A Sonic hedgehog (Shh) response element was identified in the chicken ovalbumin upstream promoter–transcription factor II (COUP-TFII) promoter that binds to a factor distinct from *Gli*, a gene known to mediate Shh signaling. Although this binding activity is specifically stimulated by Shh-N (amino-terminal signaling domain), it can also be unmasked with protein phosphatase treatment in the mouse cell line P19, and induction by Shh-N can be blocked by phosphatase inhibitors. Thus, Shh-N signaling may result in dephosphorylation of a target factor that is required for activation of COUP-TFII–, Islet1-, and Gli response element–dependent gene expression. This finding identifies another step in the Shh-N signaling pathway.

COUP-TFs belong to the orphan receptor subfamily within the steroid–thyroid hormone receptor superfamily and are found in all vertebrate species examined (*1*). In the mouse there are two COUP-TF members, COUP-TFI and COUP-TFII. Both are expressed in the neural tube during embryonic development; however, COUP-TFII is highly expressed and displays a restricted expression pattern that is coincident with motor neuron differentiation (*1*). Transplantation of a notochord to the dorsal side of the chick neural tube results in ectopic expression of COUP-TFII that coincides with the appearance of motor neuron markers such as Isl1 and SC-1 in these regions (*2*).

V. Krishnan, F. A. Pereira, Y. Qiu, S. Y. Tsai, M.-J. Tsai, Department of Cell Biology, Baylor College of Medicine, 1 Baylor Plaza, Houston, TX 77030 USA.
C.-H. Chen and P. A. Beachy, Department of Molecular Biology and Genetics, Howard Hughes Medical Institute, Johns Hopkins University, School of Medicine, Baltimore, MD 21205 USA.

*These authors contributed equally to this report.
†To whom correspondence should be addressed. E-mail: mtsai@bcm.tmc.edu

Sonic hedgehog (*Shh*) is a vertebrate homolog of the *Drosophila* segment polarity gene hedgehog (*Hh*) (*3*). The secreted Shh protein (Shh-N) from the notochord is required for induction of floor plate cells, motor neurons, and other axial midline structures (*4–7*). To investigate whether Shh activates COUP-TFII expression, we asked whether purified recombinant Shh-N expressed in *Escherichia coli* can induce COUP-TFII expression in P19 cells (*8*). Increased COUP-TFII expression is observed at Shh-N concentrations as low as 0.2 nM (Fig. 1A, lane 2). This concentration is similar to the amount that is required for regulating other Shh-N target genes (*3*, *9*) and for binding to its putative receptor, patched (*ptc*) (*10*, *11*).

To identify the target element or elements for Shh-N signaling, we used deletion analysis and identified a sequence between −1316 and −1298 nucleotides in the COUP-TFII promoter that increases reporter gene activity when linked to a heterologous herpes simplex virus thymidine kinase (*tk*) promoter (*12*) (Fig. 2). Point

mutations introduced within this element completely abolished the activation by Shh-N. Therefore, we defined this region as a Shh response element (ShhRE). Next, we examined whether this element could bind any factor or factors in response to Shh-N treatment. Nuclear extracts were prepared (*13*) from untreated P19 cells or from P19 cells treated with Shh-N and used in an electrophoretic mobility-shift assay (EMSA) (*14*). Shh-N treatment resulted in the enrichment of two specific complexes (Fig. 1B, lanes 1 and 2), which were blocked by excess ShhRE (lanes 7 to 9). Hence, Shh-N enhances the binding of a factor or factors to the ShhRE in the COUP-TFII promoter. Recent reports have identified a response element on Hh-induced target promoters that are bound by a member of the Ci/Gli family of transcription factors (*15*). The ShhRE in the COUP-TFII promoter does not resemble a Gli response element (GliRE). As expected, the GliRE is unable to compete for binding to the ShhRE in the COUP-TFII promoter (Fig. 1B, lanes 3 through 6). In contrast, in vitro translated human Gli1 can bind to the radiolabeled GliRE (*16*). Therefore, Shh signaling may not be restricted to the Ci/Gli family of transcription factors. The ShhRE includes an AT-rich motif followed by a GC core, and both are important for Shh-mediated activity. Because the binding site in the ShhRE has a TAAT motif, we predict that this element could bind to transcription factors containing a homeobox domain. Unlabeled oligonucleotide containing the Sox-9 recognition sequence is able to compete for binding to the ShhRE (*16*). Sox-9 belongs to a family of SRY-box–containing transcription factors that function in determining important cell fates during differentiation (*17*).

To address the direct or indirect nature of this Shh-mediated target response at the ShhRE, the Shh-N–induced activity of the ShhRE-linked reporter was determined in the presence or absence of cycloheximide (Chx). The Shh-induced increase in reporter mRNA synthesis was not altered by the presence of Chx (Fig. 2, compare lanes 2 and 4). In contrast, reporter enzyme activities were both inhibited (*16*). Thus, the factor(s) that binds to and activates the ShhRE is a primary target of the Shh-N signal pathway, and its activation does not require protein synthesis.

Adenosine 3′,5′-monophosphate–activated protein kinase A antagonizes Hh signaling in *Drosophila* (*1*) and in vertebrates (*18–21*). Also, the product of a *Drosophila* gene, fused (*fu*), a serine-threonine kinase, is a downstream target of Hh and is required for Hh signaling (*20, 22*). These results suggest that phosphorylation may be required for the Hh signaling pathway. Therefore, we incubated a nonspecific calf intestinal phosphatase (CIP) with both induced and uninduced nuclear extracts (Fig. 3A, lanes 5 to 8). Although incubation of CIP with Shh-N–treated extracts did not alter binding to radiolabeled ShhRE (compare lanes 7 and 8), CIP treatment of uninduced extracts was able to mimic the binding activity induced by Shh-N (compare lanes 1 and 5). Thus, the factor or factors that bind to this ShhRE are present in the nuclear extracts of untreated P19 cells, and Shh-N treatment specifically alters its ability to bind DNA by dephosphorylation.

To characterize the protein phosphatases that might mediate this activity, we used the phosphatase inhibitors okadaic acid (OA) and calyculin A (CyA) (*23*). OA is a potent inhibitor of serine-threonine–specific protein phosphatases such as PP1, PP2A, PPIV, and PPV, but it has no effect on PP2B and PP2C. OA or CyA, when treated along with Shh-N (Fig. 3B, lanes 4 and 6), resulted in complete inhibition of the induced COUP-TFII mRNA (*8*). In contrast, the inactive congener norokadone (NoA) was unable to inhibit this induction (Fig. 3B, lane 8). Similarly, OA and CyA treatment abolished the Shh-induced binding to radiolabeled ShhRE (*16*). Finally, Shh-N–mediated induction of ShhRE reporter gene activity was also shown to be completely blocked by treatment with OA (*16*). Thus, OA and CyA specifically inhibit binding of a transcription factor to the ShhRE that results in lowered promoter activity and leads to decreased COUP-TFII transcripts. To assay the direct involvement of the type of protein phosphatase in the Shh signaling pathway, we used a phosphatase assay system that quantitates the PP1 and PP2A enzyme activity in control and in Shh-N–treated nuclear extracts in the absence or presence of OA. There is a net increase (twofold) in phosphatase activity after Shh treatment that was completely abolished by OA treatment (Fig. 3C). In contrast, cotreatment with Inhibitor-2 (I-2), a specific inhibitor of PP1, does not decrease the Shh-induced phosphatase activity. Thus, it is likely that a serine-threonine phosphatase such as PP2A, PPIV, or PPV is involved in the Shh-N signaling pathway.

We tested the role of specific protein phosphatases in this pathway by transfecting P19 cells with the ShhRE-luciferase (LUC) reporter plasmid along with expression plasmids that overexpress the catalytic subunits of PP1, PP2A, PPIV, or PPV. The catalytic subunit of PP2A, when overexpressed, can mimic the activity of Shh in untreated cells [compare lanes cytomegalovirus (CMV) and PP2A in Fig. 3D] (*24*). In contrast, neither PP1, PPIV, nor PPV could mimic this activity. Thus, a PP2A-like phosphatase can mediate this Shh-induced increase in target factor activity in vivo.

To determine whether phosphatase-mediated Shh signaling extends to genes other than *COUP-TFII*, we analyzed Shh activation of Isl1 in the presence of OA (*25*). P19 cells treated with Shh-N induced Isl1 mRNA (Fig. 4A, lanes 1 and 2), and this induction was completely blocked by treatment with OA (Fig. 4A, lanes 3 and 4).

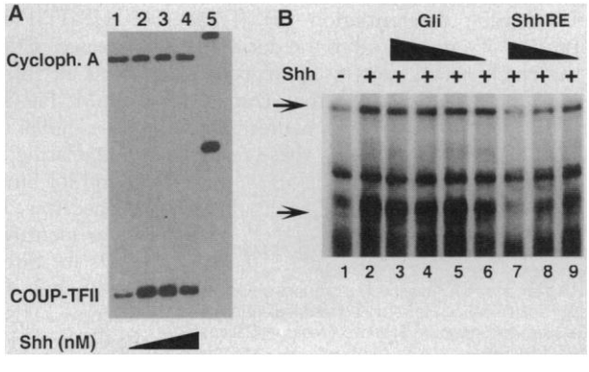

Fig. 1. Shh-induced COUP-TFII mRNA in P19 cells. (**A**) P19 cells were treated for 24 hours with 0.2 (lane 2), 0.5 (lane 3), and 1 (lane 4) nM Shh-N; total RNA was obtained for a ribonuclease protection assay as described (*13*). Murine cyclophilin A was used as a control. (**B**) P19 cells were treated with or without Shh-N for 24 hours and nuclear extracts were used in an EMSA (*20*). Different amounts of unlabeled GliRE or ShhRE (lanes 3 and 7, 100-fold excess; lanes 4 and 8, 50-fold excess; lanes 5 and 9, 25-fold excess; lane 6, 10-fold excess) were used as a competitor.

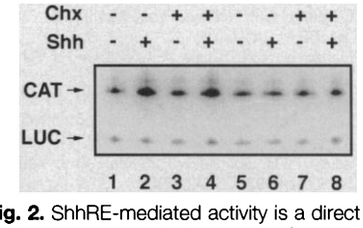

Fig. 2. ShhRE-mediated activity is a direct result of Shh-N signaling. P19 cells were cotransfected with either three copies of the ShhRE (lanes 1 to 4) or mutant ShhRE (lanes 5 to 8) tk-CAT along with tk-LUC plasmid as an internal control. Total RNA was obtained from cells pretreated with 50 μM Chx for 2 hours before addition of 1.0 nM Shh-N and harvested 12 hours later. Sixty micrograms of total RNA from these cells was used in a ribonuclease protection assay.

Furthermore, 9.5 days postcoitum (dpc) mouse neural tube explants incubated with OA exhibited decreased amounts of immunodetectable Isl1 protein (Fig. 4B) (*26*). However, this concentration of OA had no effect on the neurofilament (NFL) staining within the neural tube. Finally, the involvement of protein phosphatases in GliRE-mediated activation by Shh was tested with the GliRE reporter from the hepatocyte nuclear factor 3β 3′ enhancer (*27*). As expected, in P19 cells, the GliRE-chloramphenicol acetyltransferase (CAT) reporter was enhanced in the presence of Shh expression plasmid (Fig. 4C). This enhanced activity was also sensitive to OA treatment. These results suggest a general role for protein phosphatase in the Shh signaling pathway.

Our results indicate that the Shh-mediated mechanism of activation of the *COUP-TFII* gene may involve dephosphorylation of a factor that leads to increased binding to the ShhRE in the COUP-TFII promoter. This increase in binding resulted in enhanced COUP-TFII promoter activity. Also, the phosphatase that mediates this dephosphorylation in response to Shh-N treatment is PP2A or is like PP2A. This particular response is channeled through a protein with DNA binding activity apparently unrelated to that of the Ci/Gli family of transcription factors previously implicated in Hh signaling. A similar protein phosphatase activity is also required in the Ci/Gli-mediated branch of the *Drosophila* Hh signaling pathway (*28*). Thus, activation of specific protein phosphatase activity appears to be a general feature of Hh signal transduction.

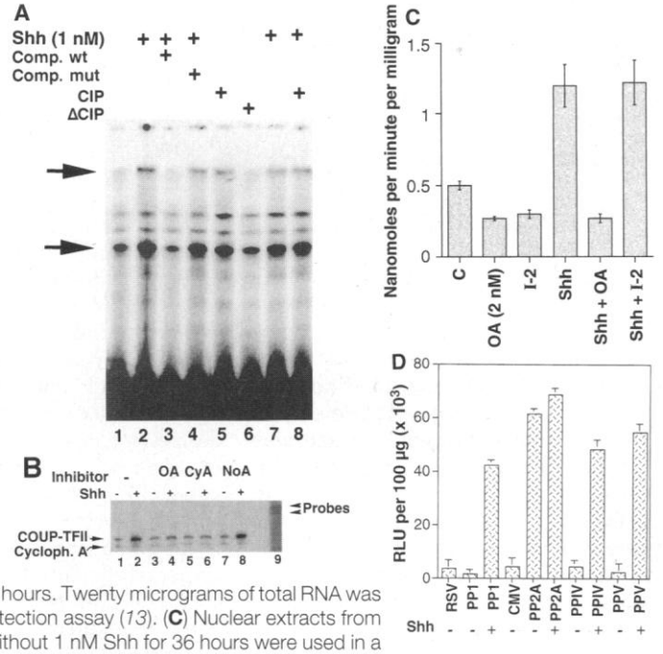

Fig. 3. Role of phosphatase in Shh-N–mediated activation of COUP-TFII. (**A**) Nuclear extracts from P19 cells treated with 1 nM Shh-N in the presence or absence of CIP or heat-denatured CIP (ΔCIP) (20 units for 15 min at room temperature) were used in an EMSA. Competitor oligonucleotides (lane 3, wild type; lane 4, mutant) were used in 100-fold molar excess. (**B**) Total RNA isolated from P-19 cells pretreated with (lanes 2, 4, 6, and 8) or without (1, 3, 5, 7, and 9) 1.0 nM Shh before addition of 5 nM OA (lanes 3 and 4), 0.5 nM CyA (lanes 5 and 6), or 5 nM NoA (lane 9) for another 12 hours. Twenty micrograms of total RNA was used in a ribonuclease protection assay (*13*). (**C**) Nuclear extracts from P19 cells treated with or without 1 nM Shh for 36 hours were used in a protein phosphatase assay system (Life Technologies, Bethesda) to quantitate the phosphatase activity with radiolabeled phosphorylase used as a substrate. In the case of inhibitors, 2 nM OA or 4 nM I-2 protein was incubated with the cells for 15 min at 30°C. (**D**) P19 cells were cotransfected with the ShhRE-SV40LUC and an expression plasmid for PP1, PP2A, PPIV, and PPV. In addition, an empty pBKRSV (RSV) or pCMV5 (CMV) vector was also cotransfected in the control wells. Cells treated with or without 1 nM Shh were harvested after 36 hours and assayed for LUC activity as described.

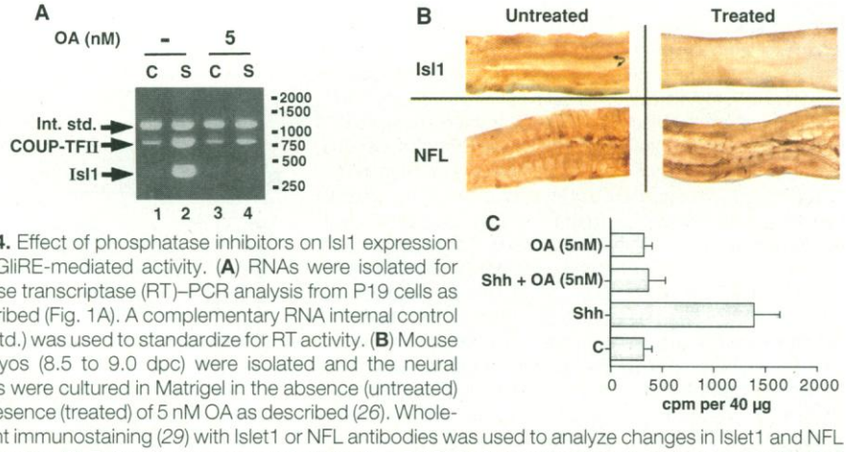

Fig. 4. Effect of phosphatase inhibitors on Isl1 expression and GliRE-mediated activity. (**A**) RNAs were isolated for reverse transcriptase (RT)–PCR analysis from P19 cells as described (Fig. 1A). A complementary RNA internal control (Int. std.) was used to standardize for RT activity. (**B**) Mouse embryos (8.5 to 9.0 dpc) were isolated and the neural plates were cultured in Matrigel in the absence (untreated) or presence (treated) of 5 nM OA as described (*26*). Whole-mount immunostaining (*29*) with Islet1 or NFL antibodies was used to analyze changes in Islet1 and NFL expression. (**C**) P19 cells were cotransfected with pBKCMV-Shh expression plasmid and a GliRE-CAT reporter plasmid (1 μg) as described (*30*). Cells cotransfected with pBKCMV-Shh (S) or pBKCMV (C) plasmid (200 ng) were treated with or without 5 nM OA for 14 hours.

REFERENCES AND NOTES

1. S.Y. Tsai and M.-J. Tsai, *Endocrine Rev.* **18**, 229 (1997).
2. B. Lutz *et al.*, *Development* **120**, 25 (1994).
3. N. Perrimon, *Cell* **80**, 517 (1995).
4. H. Roelink *et al.*, *ibid.* **76**, 761 (1994).
5. ———, *ibid.* **81**, 445 (1995).
6. Y. Tanabe, H. Roelink, T. M. Jessell, *Curr. Biol.* **5**, 651 (1995).
7. C. Chiang *et al.*, *Nature* **383**, 407 (1996).
8. Briefly, 20 μg of RNA was hybridized to a 450-nucleotide (Fig. 1A) or 120-nucleotide (Fig. 3B) riboprobe, which corresponds to the 5′ untranslated region of the *COUP-TFII* gene along with a 670-nucleotide (Fig. 1A) or 102-nucleotide (Fig. 3B) riboprobe in the murine cyclophilin A coding region. Also, a 255–base pair (bp) region of the pBLCAT2 plasmid (Bgl II–Eco RI fragment) or a 123-bp region of the LUC coding (Hinc II–Eco 1091 fragment) region was used to generate an antisense riboprobe and was hybridized with 60 μg of total RNA (Fig. 2) obtained from transfected P19 cells. The RPA II kit from Ambion was used to perform the ribonuclease (RNase) protection assay. The products were subjected to RNase digestion and analyzed on a 6% urea-polyacrylamide gel.
9. A.-H. Monsoro-Burq, M. Bontoux, C. Vincent, N. M. L. Douarin, *Mech. Dev.* **53**, 157 (1995).
10. D. M. Stone *et al.*, *Nature* **384**, 129 (1996).
11. V. Marigo, R. A. Davey, Y. Zuo, J. M. Cunningham, C. J. Tabin, *ibid.*, p. 176.
12. V. Krishnan, G. Elberg, M.-J. Tsai, S. Y. Tsai, *Mol. Endocrinol.* **11**, 1458 (1997).
13. F. J. Naya, C. M. Stellrecht, M.-J. Tsai *Genes Dev.* **9**, 1009 (1995).
14. Radiolabeled probe (40 pg) was incubated with the nuclear extracts (10 μg) along with 4 μg of poly(dG-dC) in a binding reaction mixture containing 10 mM tris (pH 7.5), 50 mM NaCl, 1 mM EDTA, 1 mM dithiothreitol, 0.1 mg of bovine serum albumin per milliliter, and 5% (v/v) glycerol. Later the mixture was loaded onto a 5% polyacrylamide gel and the retarded complexes were separated in 1× tris-borate EDTA buffer and analyzed by autoradiography. The following oligonucleotides were used as competitors or probes in these assays: wild type or ShhRE, GTTCTACATAATGCGCCG; mutant, TTCTACgTgATGCGCCG; GliRE, TCCCGAAGACCACCCACAATGA.
15. C. Alexandre, A. Jacinto, P. W. Ingham, *Genes Dev.* **10**, 2003 (1996).
16. V. Krishnan *et al.*, data not shown.
17. L. H. Pevny and R. Lovell-Badge. *Curr. Opin. Genet. Dev.* **7**, 338 (1997).
18. J. P. Concordet *et al.*, *Development* **122**, 2835 (1996).
19. C. M. Fan *et al.*, *Cell* **81**, 457 (1995).
20. M. Hammerschmidt, M. J. Bitgood, A. P. McMahon, *Genes Dev.* **10**, 647 (1996).
21. M. Hynes *et al.*, *Neuron* **15**, 35 (1995).
22. P. P. Therond, J. D. Knight, T. B. Komberg, J. M. Bishop, *Proc. Natl. Acad. Sci. U.S.A.* **93**, 4224 (1996).
23. P. Cohen, *Annu. Rev. Biochem.* **58**, 453 (1989).
24. P19 cells were transfected with a plasmid encoding three copies of the ShhRE, placed upstream of a simian virus 40 LUC plasmid (3 × ShhRE-

SV40LUC). Also, a pBKRSV, pCMV4, Rous sarcoma virus (RSV)–PP1, CMV-PP2A, CMV-PPIV, or CMV-PPV expression plasmid was cotransfected along with the reporter plasmid. Cells were treated with 1 nM Shh and assayed for reporter gene activity.

25. An internal control containing a 763-bp insert into the Sph I site of the Islet1 cDNA was transcribed in vitro to prepare sense-oriented RNA. One nanogram of this RNA along with 100 ng of total RNA from appropriately treated P19 cells was reverse transcribed using Superscript II, and 1/10th of each reaction mixture was amplified by polymerase chain reaction (PCR). Specific primers for Islet1 (forward primer, 5′ TCA AAC CTA CTT TGG GGT CTT A 3′; reverse primer, 5′ ATC GCC GGG GAT GAG CTG GCG GCT 3′) and for COUP-TFII (forward primer, 5′ GAT ATG GCA ATG GTA GTC AGC ACG TGG 3′; reverse primer, 5′ AGC TTC TCC ACT TGC TCT TGG 3′) were used for PCR amplification (94°C for 1 min, 54°C for 1 min, and 72°C for 1 min). Twenty-two cycles were used for amplifying Islet1 and the resulting products were separated on a 1% agarose gel in tris-acetate EDTA (TAE) buffer. A 427-bp Isl1 fragment and an 838-bp COUP-TFII fragment were used to estimate changes in mRNA quantities.
26. Mouse embryos at embryonic day 9 to 9.5 were dissected in such a way as to remove surface ectoderm and somitic mesoderm, and neural tubes were isolated from the level of rhombomere 8 in the rostral region to the first segmenting somite in the caudal region. Neural tubes were cultured for 24 hours dorsal side down on Millicell-CM membranes and overlaid with Matrigel containing 10 ng of NT-3 per milliliter, with L15 air medium (*4*) in the presence or absence of 5 nM OA. The explants were subjected to whole-mount immunostaining with a monoclonal antibody raised against mouse Islet1 (39.4D5) or NFL (2H3) as described (*29*).
27. H. Sasaki, C.-C. Hui, M. Nakafuku, H. Kondoh, *Development* **124**, 1313 (1997).
28. C-H. Chen, N. Fuse, P. A. Beachy, personal communication.
29. M. C. Mumby and G. Walter, *Physiol. Rev.* **73**, 673 (1993).
30. C. M. Gorman, L. F. Moffat, B. H. Howard, *Mol. Cell. Biol.* **2**, 1044 (1982).
31. Purified Shh-N was provided by J. A Porter and K. Young, purified protein phosphatases PP1 and PP2A were provided by S. Shenolikar (Duke University), PPIV protein and expression plasmid were provided by T-H. Tan (Baylor College of Medicine). CMV-PPV plasmid was provided by M. Chinkers (Oregon University, Health Science Center). PP1 and PP2A expression plasmids were kindly provided by T. Deng (University of Florida). Human Gli and GliRE-CAT reporters were provided by C-C. Hui (University of Toronto, Canada). The authors also wish to thank N. Fuse for communication of unpublished results. This work is supported by an NIH grant.

6 June 1997; accepted 3 November 1997

Spike Synchronization and Rate Modulation Differentially Involved in Motor Cortical Function

Alexa Riehle,* Sonja Grün, Markus Diesmann, Ad Aertsen

It is now commonly accepted that planning and execution of movements are based on distributed processing by neuronal populations in motor cortical areas. It is less clear, though, how these populations organize dynamically to cope with the momentary computational demands. Simultaneously recorded activities of neurons in the primary motor cortex of monkeys during performance of a delayed-pointing task exhibited context-dependent, rapid changes in the patterns of coincident action potentials. Accurate spike synchronization occurred in relation to external events (stimuli, movements) and was commonly accompanied by discharge rate modulations but without precise time locking of the spikes to these external events. Spike synchronization also occurred in relation to purely internal events (stimulus expectancy), where firing rate modulations were distinctly absent. These findings indicate that internally generated synchronization of individual spike discharges may subserve the cortical organization of cognitive motor processes.

The classical view of neural coding has emphasized the importance of information carried by changes in the neurons' spike discharge rates (*1*). Thus, relating rate changes of individual neurons to cognitive and motor functions has yielded remarkable insights into neuronal mechanisms of sensory (*2*) and motor (*3*) processing. In parallel, however, the concept emerged that computational processes in the brain could also rely on the relative timing of spike discharges among neurons within functional groups (*4*)—commonly called cell assemblies (*5*). Indeed, it has been argued that the synaptic influence of multiple neurons converging onto others is much stronger if they fire in coincidence (*6*), making synchrony of firing ideally suited to raising the saliency of responses and to expressing relations among neurons with high temporal precision (*4*). For this temporal scheme to work, correlations in spike timing must reflect cooperative interactions among the neurons constituting an assembly. Moreover, to permit neurons to participate in different cell assemblies at different times, depending on the present stimulus context and behavioral demands, these correlations should be dynamic. Indeed, such predicted stimulus- and behavior-dependent modulations of spike correlations with differing degrees of temporal precision were observed in various sensory cortical areas, particularly visual (*7*), auditory (*8*), somatosensory (*9*), and frontal (*10*) areas. However, very little is known about the possible functional role of action potential timing in the motor cortex (*11*), in spite of the fact that this part of the brain directly governs overt behavior. We present evidence for the hypothesis that precise synchronization of individual action potentials among selected groups of motor cortex neurons is involved in dynamically organizing the cortical network dur-

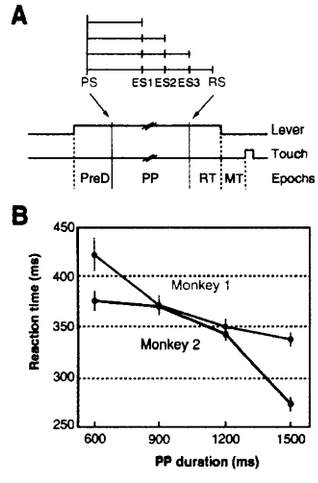

Fig. 1. (**A**) Two macaque monkeys were trained to touch a target presented on a video display equipped with a capacitive touch screen. To start a trial, the animal had to hold down a switch. After a constant delay of 1 s (PreD), a PS forming an open circle (diameter, 3 cm) appeared on the screen, indicating the upcoming target position. After a second delay of variable duration (PP), the RS, indicated by filling the circle, instructed the animal to move its hand to the target and touch it. The PP could last 600, 900, 1200, or 1500 ms; these intervals were presented in random order and with equal probability. Thus, from one possible PP duration (and, hence, ES) to the next, the conditional probability for the RS to occur increased, reaching values of 0.25, 0.33, 0.5, and 1. RT and movement time (MT) were recorded in each trial. Criteria for obtaining the reward were (1) to keep the switch pressed during the PP, (2) to move to and touch the target after RS, and (3) to perform the movement so that neither RT nor MT exceeded 1 s. (**B**) Behavioral results. For each monkey, mean RTs and standard error in relation to PP duration are shown as recorded during the last training sessions (monkey 1, $N = 35$; monkey 2, $N = 59$) when they performed the task with more than 90% correct trials. By using a two-factor (PP duration × training session) analysis of variance, changes in RT were found to be highly significant for both monkeys [monkey 1, $F(3,102) = 38.19$, $P < 0.001$; monkey 2, $F(3,174) = 157.81$, $P < 0.001$].

A. Riehle, Center for Research in Cognitive Neuroscience, CNRS, 31 Chemin Joseph Aiguier, 13402 Marseille Cx 20, France.
S. Grün, Department of Physiology, The Hebrew University, Hadassah Medical School, Jerusalem 91120, Israel. E-mail: gruen@hbf.huji.ac.il
M. Diesmann and A. Aertsen, Department of Neurobiology and Biophysics, Institute of Biology III, Albert-Ludwigs-University, Schänzlestrasse 1, D-79104 Freiburg, Germany. E-mail: diesmann@biologie.uni-freiburg.de and aertsen@biologie.uni-freiburg.de

*To whom correspondence should be addressed. E-mail: ariehle@lnf.cnrs-mrs.fr